

Thermodynamic Performance and Components Cost Analysis for a Low Enthalpy Geothermal Power Plant

Antonios Iasonas S. Karypidis^a, Dimitrios K. Misirlis^{a,*}, Christiana M. Papapostolou^b, Kostas D. Kleidis^a

^aDept. of Mechanical Engineering, International Hellenic University, Terma Magnesias, 62124, Serres, Greece

^bDept. of Mechanical Engineering, University of West Attica, 250 Thivon & P. Ralli Str, Egaleo, 12241, Athens, Greece

dmissirlis@ihu.gr

This work presents an analysis of the effect of different working fluids on the thermodynamic performance and components cost distribution for a low enthalpy geothermal binary cycle power plant. The assessment of the purchase cost of the main cycle components was based on dedicated correlations from international literature, that correlate the components purchase cost to their primary operational characteristics, such as power and the UA parameter. The analysis was focused on two different working fluids, R134a and sCO₂ for the conditions of the low enthalpy geothermal fields, of Sidirokastron, Serres, Greece and Chena, Alaska, USA to compare the combined effect of different geothermal source temperature, condensation temperature and working fluids on thermodynamic performance and purchase cost of binary cycle components. The purchase cost analysis for sCO₂ as working fluid identified the most cost intensive components with the water condenser cost being the higher at ~28-33 % of the total purchase cost followed by the geothermal heat exchanger at ~22-23 %. Furthermore, the use of sCO₂ led to increased UA values ranging from ~12 % to ~45 % resulting to noticeable cost increase. As a result, the analysis showed that the use of sCO₂ results in a significant cost increase in relation to R134a ranging from 19.33 % when dry cooling is used up to 42.58 % when water condenser is selected. For these reasons, combined modifications were introduced and assessed in the sCO₂ binary cycle with preheating, reheating and intermediate heat transfer through which ~12 % cost reduction was achieved, covering a significant part of the cost difference between the two working fluids.

1. Introduction

Various research activities and initiatives, e.g. the European Green Deal (European Commission, 2022) have appeared targeting the achievement of climate neutrality and zero emissions of greenhouse gases by 2050. To this direction a large number of activities is focused on the utilization of low-enthalpy geothermal energy sources, since the latter compose more than 40 % of the total geothermal energy potential in the South-East Europe (Sigfusson and Uihlein, 2016) including also Greece (Papachristou et al., 2021). The proper estimation of the low enthalpy geothermal energy benefits should also include cost-related economic aspects taking into consideration the effects of working fluid selection and geothermal field characteristics that can have a critical impact on optimal system design, thermodynamic performance and cost (Lee and Chen, 2022).

The selection of working fluids is of critical importance especially when parameters such as GWP or ODP are considered. Currently, fluids such as R134a, R236ea, R236fa, R245fa, and R142b appear as suitable for low enthalpy applications between 50 -100 °C (Thurairaja et al. 2019) among others. However, when stricter environmental parameters are applied concerns about their use appear since one of their GWP and ODP values is relatively high. Furthermore, taking into consideration the possible hydrofluorocarbon (HFC) phase-down in Europe planned for 2030, (EEA, 2025), since HFCs account for the majority of fluorinated greenhouse gases emissions, and their replacement with clean, environmentally friendly and non-toxic fluids, the consideration of less conventional fluids such as CO₂ which has GWP=1 and ODP=0 becomes more interesting. Thus, the quantification of the effect of using fluids such as sCO₂ in relation to fluids such as R134a, to thermodynamic performance and components cost can be of high importance.

Such an effort is presented in this work. The main part of the analysis was focused on the conditions of the low enthalpy geothermal field in Sidirokastron, Serres, Greece, which provides geothermal water of $T_{max}=78\text{ }^{\circ}\text{C}$. targeting 250 kW of power generation. Furthermore, a thermodynamic analysis corresponding to the conditions of the low enthalpy geothermal field in Chena, Alaska, USA of $T_{max}\sim 74\text{ }^{\circ}\text{C}$ and low condensation temperature was performed to assess the combined effect of different conditions on both thermodynamic performance and purchase cost. The analysis identified the most important cycle components from a cost-intensive point of view and revealed the effect of working fluid and operating conditions on performance and cost. Finally, new modifications were introduced in the basic $s\text{CO}_2$ binary cycle to improve efficiency and reduce its cost, in relation to R134a, through the combined use of preheating, reheating and intermediate heat transfer.

2. Methods

2.1 Thermodynamic model development

The thermodynamic analysis was performed with two open-source software tools, the Cape Open to Cape Open COCO simulator (COCO, 2025) and the DWSIM – Open-Source Chemical Process Simulator (DWSIM, 2025). The performance of DWSIM and COCO was assessed in various works in relation to commercial software showing close agreement as shown in the work of Tangsriwong et al. (2020) among others.

The geothermal power plant model is shown in Figure 1a. The binary cycle components characteristics were based on open-literature data and more specifically, for the Chena power plant conditions ($T_{max}=73.33\text{ }^{\circ}\text{C}$, 33.39 kg/s, $T_{cool}=4.44\text{ }^{\circ}\text{C}$) on the work of Aneke et al. (2011) and for the Sidirokastron conditions ($T_{max}=78\text{ }^{\circ}\text{C}$, 31.95 kg/s, $T_{cool}=8\text{ }^{\circ}\text{C}$) on the work of Chassapis et al. (2019), as updated by Karypidis et al. (2025). For the $s\text{CO}_2$ thermophysical properties, the Peng Robinson (1976) equation of state was used while for R134a the CoolProp library (Bell et al., 2014) as implemented in DWSIM, was used. The selection of Peng-Robinson EOS was based on the conclusions of Atinga (2024) when this EOS was used for modelling the $s\text{CO}_2$ thermophysical properties in ASPEN software. The modelling equations and assumptions are shown in Table 1.

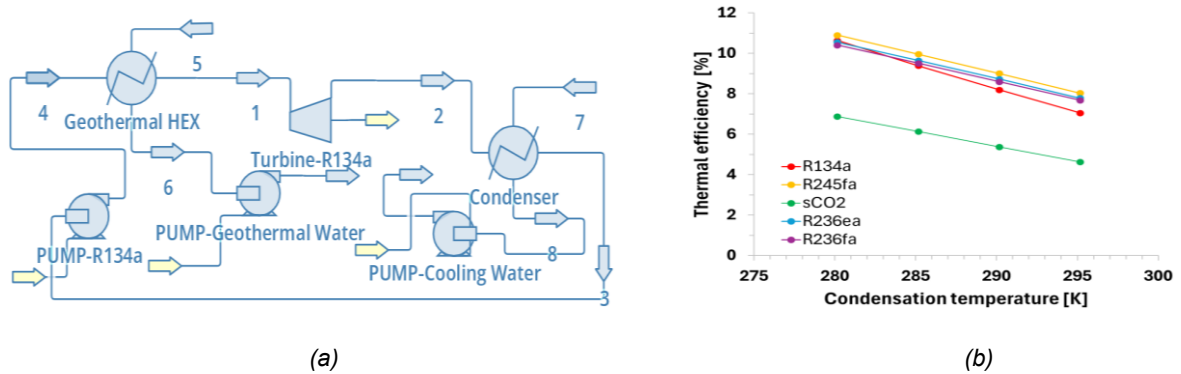


Figure 1: (a) Geothermal power plant model (in DWSIM); (b) Thermal efficiency vs conditions.

Table 1: Thermodynamic equations and assumptions applied

Components	Equations and assumptions
GHEX	$\dot{Q}_{GHEX} = \dot{m}_{working\ fluid}(h_1 - h_4) = \dot{m}_{geothermal\ water}(h_5 - h_6)$
Turbine	$\dot{W}_t = \dot{m}_{working\ fluid}(h_1 - h_2)$
Condenser	$\dot{Q}_{cond} = \dot{m}_{working\ fluid}(h_2 - h_3) = \dot{m}_{cooling\ water}(h_8 - h_7)$
Pump working fluid	$\dot{W}_p = \dot{m}_{working\ fluid}(h_4 - h_3)$
Turbine isentropic efficiency	80 %
Pump efficiency isentropic	80 %
HEXs (GHEX, Condenser)	effectiveness 95 %, saturated liquid at condenser outlet
Geothermal water temperature drop	$\sim 20\text{ }^{\circ}\text{C}$

2.2 Components cost models

An assessment of the purchase cost of the main components of the geothermal binary cycle power plant using $s\text{CO}_2$ was performed based on correlations from international literature. These dedicated cost functions were

based on the works of Weiland et al. (2019), Towler et al. (2021), Bleich and Bleich (2023), McCollum and Ogden (2006) and Shamoushaki et al. (2021), as shown in Table 2 and correlate the purchase cost of these components to their primary operational characteristics, such as power and UA parameter (the product of overall heat transfer coefficient and heat exchanger surface area).

For the more accurate calculation of the UA parameter of the heat exchangers detailed sub-models of the geothermal heat exchanger (GHEX) and the condenser were developed to properly capture the effect of the working fluid thermophysical properties variations in specific enthalpy and specific heat capacity, to the calculation of the logarithmic mean temperature difference and to the UA parameter value. These sub-models were developed with COCO simulator on which the heat exchange process was divided into 20 internal sub-processes of equal heat transfer and the total UA value was calculated as the sum of the UA values of each one of the internal heat exchange steps, taking into account the conclusions of Karypidis et al. (2025).

Table 2: Geothermal power plant main components cost functions

Component	Cost model	Scale parameter	Reference
GHEX	$49.45 \cdot (UA)^{0.7544}$	UA [W/K]	Weiland et al. (2019)
	$(-0.06395 \cdot A^2 + 947.2P + \log A + 227.9) \cdot f_m \cdot f_p$	A [m ²]	Towler et al. (2021) and Bleich and Bleich (2023)
Turbine	$406200 \cdot (P^{0.8})$	P [MW]	Weiland et al. (2019)
Condenser	$C \cdot 49.45 \cdot (UA)^{0.7544}$	UA [W/K]	Weiland et al. (2019)
	$(-0.06395 \cdot A^2 + 947.2P + \log A + 227.9) \cdot f_m \cdot f_p$	A [m ²]	Towler et al. (2021) and Bleich and Bleich (2023)
Dry Cooler	$32.88 \cdot (UA)^{0.75}$	UA [W/K]	Weiland et al. (2019)
sCO ₂ Pump	$(1.11 \cdot 10^6) \cdot (P/1000) + 0.07 \cdot 10^6$	P [kW]	McCollum and Ogden (2006)
	$(-0.03195 \cdot P^2 + 467.2P + \log P + 20480) \cdot f_m \cdot f_p$	P [kW]	Towler et al. (2021) and Bleich and Bleich (2023)
Pumps	$(-0.03195 \cdot P^2 + 467.2P + \log P + 20480) \cdot f_m \cdot f_p$	P [kW]	Towler et al. (2021) and Bleich and Bleich (2023)
Cooling Tower	$1500 \cdot (V^{0.9}) + 170000$	Volume flow rate [l/s]	Shamoushaki et al. (2021) and Bleich and Bleich (2023)

3. Results and Discussion

The DWSIM model of the Chena power plant was used to perform a direct comparison with the results of Aneke et al. (2011), derived with the use of the commercial SimTech IPSEpro Simulation Software (SimTech, 2008). A detailed comparison is shown in Table 2 where a close agreement is presented having a deviation of 0.01 % on the thermal efficiency and of ~0.1 kW on the net power. The comparison is based on the thermodynamic cycle data as included in Aneke et al. (2011) and thus, a thermal efficiency of 9.47 % is used as the reference value even though the actual cycle efficiency is ~8.2 % when other auxiliary power consumptions and losses are considered. A similar analysis was also performed with DWSIM and COCO simulator models for Chena and Sidirokastron geothermal field conditions using R134a and sCO₂ as working fluids, as shown in Tables 3 and 4.

Table 3: Comparison of Chena geothermal field conditions models using R-134a and sCO₂

Parameter	IPSEpro	DWSIM R-134a	DWSIM sCO ₂	COCO sCO ₂
Q _{GHEX} (kW)	2,571.48	2,570.88	2,594.01	2,593.77
Q _{cond} (kW)	2,328	2,327.68	2,434.66	2,436.14
W _t (kW)	265.8	265.70	271.72	271.92
W _p (kW)	22.32	22.51	112.39	114.29
W _{net} (kW)	243.48	243.19	159.33	157.63
n _{th} (%)	9.47	9.46	6.14	6.08
Fluid mass flow rate (kg/s)	12	12	13.2	13.2
Pressures max-min (bar)	17.85-4.38	17.85-4.38	100-47.02	100-47.02

The use of R134a provides significant advantage both in terms of thermal efficiency and net power of the power plant cycle. For Chena conditions the use of R134a provides a thermal efficiency of 9.46 % while the use of sCO₂ limits the cycle thermal efficiency to 6.14 % for the DWSIM model and 6.08 % for the COCO model. The use of R134a provides cycle net power of ~243 kW while the use of sCO₂ limits the cycle net power to ~159 kW for the DWSIM model and ~158 kW for the COCO model. As a result, R134a provides a relative improvement

in relation to sCO₂ of ~54 % for the thermal efficiency (net improvement of ~3.3 %) and ~52 % for the net power of the binary cycle (net improvement of ~84 kW).

For Sidirokastron conditions a similar trend appears since R134a provides a thermal efficiency of 10.01 % while sCO₂ of ~5.53 % for the DWSIM model and ~5.46 % for the COCO model. The use of R134a provides a cycle net power of ~459 kW while sCO₂ of ~254 kW for the DWSIM model and ~250 kW for the COCO model. The use of R134a provides a relative improvement in relation to sCO₂ of ~80 % for the thermal efficiency (net improvement of ~4.5 %) and ~81 % for the net power (net improvement of ~204 kW). The sCO₂ thermal efficiency comparison in relation to other working fluids, i.e. R134a, R236ea, R236fa, R245fa, for varying T_{cool}, presents similar performance, shown in Figure 1b, based on the assumptions of Table 1 with the cycle maximum pressure being selected in order to achieve the same temperature and degree of superheat in turbine inlet.

In all these comparisons, the mass flow rate of the working fluid was adjusted in order to extract the same thermal power from the geothermal source taking as reference a) for the Chena geothermal field the thermal power extracted by R134a in the work of Aneke et al. (2011) and b) for the Sidirokastron geothermal field the thermal power extracted by the sCO₂, as mentioned in Karypidis et al. (2025).

Regarding the simulations, as shown in Tables 3 and 4, the comparison of the DWSIM results in relation to the results of Aneke et al. (2011) which were derived with the use of the commercial SimTech IPSEpro Simulation Software (SimTech, 2008) present a relative difference of ~0.1 % for the thermal efficiency and ~0.3 % for the UA value while the DWSIM and COCO results present a relative difference of ~1.3 %.

Based on these results an assessment of the purchase cost distribution of the main components of the geothermal binary cycle power plant was performed as presented in Table 5 where the total components costs of the sCO₂ geothermal power plant for both the Sidirokastron and Chena geothermal field conditions are presented in relation to the total cost of the Chena R134a geothermal power plant based on the best available information, Holdmann (2008).

Table 4: Comparison of Sidirokastron geothermal field conditions models using R-134a and sCO₂

Parameter	DWSIM R-134a	DWSIM sCO ₂	COCO sCO ₂
Q _{GHEX} (kW)	4,587.36	4,599.72	4,586.15
Q _{cond} (kW)	4,128.08	4,345.26	4,335.85
W _t (kW)	487.40	425.24	425.33
W _p (kW)	28.14	170.80	175.03
W _{net} (kW)	459.26	254.44	250.30
n _{th} (%)	10.01	5.53	5.46
Fluid mass flow rate (kg/s)	21.04	22.22	22.22
Pressures max-min (bar)	17.85-4.43	100-51.96	100-51.96

Table 5: Components cost distribution and total costs comparison for the geothermal binary cycle power plant

Component	Sidirokastron with sCO ₂	Chena with sCO ₂
GHEX	23.05 %	21.85 %
Turbine	7.17 %	8.10 %
Water Condenser	32.44 %	27.72 %
Pump sCO ₂	11.21 %	13.49 %
Pumps	3.30 %	2.20 %
Cooling Tower	12.26 %	13.47 %
Sum of Gearbox, Generator, Motors	10.58 %	13.16 %
Relative total purchase cost vs Chena plant with R134a for weighted net power	+47.26 %	+42.58 % (using Water condenser) +19.33 % (using Dry Cooler)

Table 6: Comparison of UA values for different working fluids and conditions

Component	Chena with R134a	Chena with sCO ₂	Sidirokastron with sCO ₂
GHEX	119.3 kW/K (for 2571.5 kW)	144.6 kW/K (for 2593.8 kW)	293.35 kW/K (for 4586.2 kW)
Difference	- (119.2 for DWSIM)	+21.23 %	+37.87 % (kW weighted value)
Condenser	336.0 kW/K (for 2328 kW)	378.4 kW/K (for 2436.1 kW)	908.28 kW/K (for 4335.9 kW)
Difference	- (337.1 for DWSIM)	+12.61 %	+45.14 % (kW weighted value)

All components cost correspond to USD\$-2017 and for translating them to current year USD\$ cost levels the CECPI index can be applied, as mentioned in Weiland et al. (2019), where the CECPI 2017 index was 567.5.

Furthermore, the UA values comparison for R134a and sCO₂ are shown in Table 6. The use of sCO₂ results to increased UA values ranging from 12 % to 45 % (the latter for higher T_{cond}) and noticeable increase of the total purchase cost of the components since the selection of R134a allows the use of lower cost commercially available components and low cost HEXs, as mentioned in Holdmann (2008).

At the present paper the main source of correlations is the work of Weiland et al. (2019) where CO₂ specific cost correlations were developed collaboratively from an aggregate set of vendor quotes, cost estimates, and published literature. The cost of GHEX, condenser and sCO₂ pump, which are the most expensive components, were assessed with two cost correlations. The GHEX and condenser cost correlations of Weiland et al. (2019) were compared to the ones of Towler et al. (2021) and Blecich and Blecich (2023) showing +7 % relative cost difference for the GHEX and +5 % for the condenser in relation to Weiland et al. (2019) and +11 % for the sCO₂ pump cost in relation to McCollum and Ogden (2006).

Lowering sCO₂ related costs is of high importance to consider sCO₂ as alternative fluid. For this reason, the integration of cycle modifications, such as the ones in Figure 2, should be assessed which include:

- the use of additional heat sources, i.e. solar collectors, after GHEX to increase cycle temperature (in R-4)
- the application of solar collectors for preheating before GHEX to increase cycle power potential (in R-2)
- the use of intermediate HEX to reduce the condenser load and preheat fluid before GHEX (in R-1)
- the use of absorption chillers to reduce and control the condensation temperature (in R-3)
- the partial use of dry cooling to reduce cost and water cooler size (in R-3)

An equivalent model of the enhanced thermodynamic cycle was created for the conditions of Chena geothermal field. The main components characteristics were based on the assumptions of Table 1 while the ones for the solar preheater and reheater and the intermediate HEX, were based on the work of Chassapis et al. (2019). The analysis showed that the use of solar preheating to 35-45 °C and solar reheating up to 90 °C, together with the use of intermediate HEX of 90 % effectiveness leads to 10.7-11.6 % cost decrease and more than 25 % efficiency increase for similar net power showing the benefits of the adapted modifications. These modifications when dry cooling is applied, reduce the cost difference to the one of Chena R134a power plant to +11.2 %.

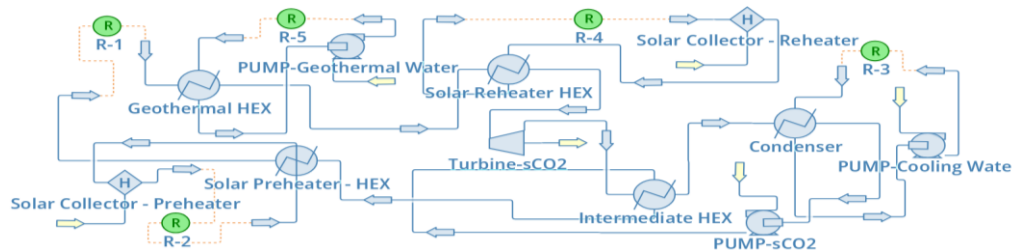


Figure 2: Enhanced cycle modifications setup in DWSIM

4. Conclusions

In all examined cases the thermodynamic performance of R134a was better than the one of sCO₂ in terms of thermal efficiency and net power by more than 50 %. The combined cost of the GHEX and the condenser was higher than ~50-55 % of the total purchase cost of the sCO₂ binary cycle components with the water condenser cost being the highest at ~28-33 %, followed by the GHEX at ~22-23 %.

The use of sCO₂ led to increased UA values ranging from 12 % to 45 % resulting to noticeable cost increase. As a result, the analysis showed that the use of sCO₂ results in a significant cost increase in relation to R134a ranging from 19.33 % when dry cooling is used up to 42.58 % when water condenser is selected. This significant cost increase can be also partially attributed to the more effective thermophysical properties of R134a that facilitate an efficient turbine expansion process and a much more effective than sCO₂ pump operation of less power consumption, increased net power and increased thermal efficiency. Furthermore, the Chena conditions power plant with sCO₂ and water condenser uses increased water flow rate in relation to Chena conditions power plant with R134a. Finally, modifications were introduced in the sCO₂ binary cycle with the use of preheating, reheating and intermediate heat transfer which led to ~12 % cost reduction and more than 25 % relative efficiency increase covering a significant part of the cost difference in relation to R134a. These results will be included in a technoeconomic analysis that will follow.

Nomenclature

A – Heat exchanger area, m²

C – material thickness correction term

h – Specific enthalpy, kJ/kg

f_m – material correction factor

f_p – pressure correction factor

GHEX – Geothermal heat exchanger

GWP- Global Warming Potential	T_{cool} – Cooling water temperature, °C
HEX – Heat exchanger	T_{max} – Geothermal water temperature, °C
m – mass flow rate	UA – Heat conductance, W/K
n_{th} – Thermal efficiency	U – Overall heat transfer coefficient, W/(m ² K)
ODP - Ozone Depletion Potential	V - Volumetric flow rate, l/s
P – Power	W_{net} – Net power
Q_{cond} – Condenser thermal power	W_p – Pump power
Q_{GHEX} – Geothermal heat exchanger power	W_t – Turbine power
sCO ₂ - supercritical carbon dioxide	

References

- Aneke M., Agnew B., Underwood C., 2011, Performance Analysis of the Chena Binary Geothermal Power Plant. *Applied Thermal Engineering*, 31, 1825-1832.
- Bell I.H., Wronski J., Quoilin S., Lemort, V., 2014, Pure and Pseudo-pure Fluid Thermophysical Property Evaluation and the Open-Source Thermophysical Property Library CoolProp. *Industrial and Engineering Chemistry Research*, 53, 2498–2508.
- Blecich A.A., Blecich P., 2023, Thermo-economic Analysis of Subcritical and Supercritical Isobutane Cycles for Geothermal Power Generation. *Sustainability*, 15, 8624.
- Chasapis D., Misirlis D., Papadopoulos P.A., Kleidis K., 2019, Thermodynamic Analysis on the Performance of a Low-Enthalpy Geothermal Field Using a CO₂ Supercritical Binary Cycle. *Chemical Engineering Transactions*, 76, 1009-1014.
- COCO, 2024, The CAPE-OPEN simulator, <www.cocosimulator.org/index.html>, accessed on 24.04. 2025.
- DWSIM, 2025, The Open Source Chemical Process Simulator, <dwsim.org/>, accessed 24.04.2025.
- European Environment Agency (EEA), 2025, Hydrofluorocarbon phase-down in Europe, <eea.europa.eu/en/analysis/indicators/hydrofluorocarbon-phase-down-in-europe>, accessed 05.06.2025.
- European Commission, 2022, A European Green Deal: Striving to be the First Climate-Neutral Continent. <https://commission.europa.eu/strategy-and-policy/priorities-2019-2024/european-green-deal_en>, accessed 24.04.2025.
- Holdmann G., 2008, The Chena Hot Springs 400 kW Geothermal Power Plant: Experience Gained During the First Year of Operation. *Transactions-Geothermal Resources Council*, 31, 515-519.
- Karypidis A.I., Misirlis D., Papapostolou C., Kleidis K., 2025, Preliminary Analysis of Components Cost Distribution for a Low Enthalpy Geothermal Power Plant. *International Conference on Renewable Energy Systems with Focus on Solar Technologies*, Thessaloniki, Greece, April 09–11.
- Lee J.-Y., Chen S.-L., 2022, Optimal Design of a Geothermal Organic Rankine Cycle System. *Chemical Engineering Transactions*, 94, 523-528.
- McCollum D.L., Ogden J.M., 2006, Techno-Economic Models for Carbon Dioxide Compression, Transport, and Storage and Correlations for Estimating Carbon Dioxide Density and Viscosity. UC Davis: Institute of Transportation Studies, University of California, Davis, USA, UCD-ITS-RR-06-14.
- Papachristou M., Dalampakis P., Arvanitis A., Mendrinis D., Andritsos N., 2021. Geothermal developments in Greece – Country update 2015-2020, *World Geothermal Congress*, Reykjavik, Iceland, April - October 2021
- Peng D.Y., Robinson D.B., 1976, A New Two-Constant Equation of State. *Industrial and Engineering Chemistry Fundamentals*, 15, 59–64.
- Shamoushaki M., Niknam P.H., Talluri L., Manfrida G., Fiaschi D., 2021, Development of Cost Correlations for the Economic Assessment of Power Plant Equipment. *Energies*, 14, 2665.
- Sigfusson B., Uihlein A., 2016, 2015 JRC Geothermal Energy Status Report. European Commission Joint Research Centre, EUR 27623 EN.
- SimTech, IPSEpro PSE version 4.0, SimTech Simulation Technology, 2008, <www.simtechnology.com>, accessed 04.06.2025.
- Tangsrivong K., Lapchit P., Kittijungjit T., Klamrassamee T., Sukjai Y., Laonual Y., 2020, Modeling of chemical processes using commercial and open-source software: A comparison between Aspen Plus and DWSIM. *IOP Conference Series: Earth and Environmental Science*, 463, 012057.
- Thurairaja K., Wijewardane A., Jayasekara S., Ranasinghe C., 2019. Working Fluid Selection and Performance Evaluation of ORC. *Energy Procedia*, 156, 244-248.
- Towler G., Sinnott R. (Eds), 2021, *Chemical Engineering Design: Principles, Practice and Economics of Plant and Process Design*, 3rd ed., Butterworth-Heinemann (Elsevier), Oxford, UK.
- Weiland N.T., Lance B.W., Pidaparti S.R., 2019, sCO₂ Power Cycle Component Cost Correlations from DOE Data Spanning Multiple Scales and Applications. *Proceedings of ASME Turbo Expo 2019: Turbomachinery Technical Conference and Exposition*. Volume 9. Phoenix, Arizona, USA. June 17–21, GT2019-90493.